

# Diphoton production at Next-to-Next-to-Leading-Order

Leandro Cieri<sup>a</sup>

<sup>a</sup>*INFN, Sezione di Firenze,  
Via G.Sansone 1, I-50019 Sesto Fiorentino, Florence, Italy.*

---

## Abstract

We consider direct diphoton production in hadron collisions. We compute the next-to-next-to-leading order (NNLO) QCD radiative corrections at the fully-differential level. Our calculation uses the  $q_T$  subtraction formalism and it is implemented in a parton level Monte Carlo program, which allows the user to apply arbitrary kinematical cuts on the final-state photons and the associated jet activity, and to compute the corresponding distributions in the form of bin histograms. We present selected numerical results related to Higgs boson searches at the LHC and the Tevatron, and we show how the NNLO corrections to diphoton production are relevant to understand the main background of the decay channel  $H \rightarrow \gamma\gamma$  of the Higgs boson  $H$ .

**Keywords:** QCD, NNLO, Diphoton, Higgs

---

## 1. Introduction

Diphoton production is a relevant process in hadron collider physics. It is both a classical signal within the Standard Model (SM) and an important background for Higgs boson and new-physics searches. The origin of the Electroweak symmetry breaking is currently being investigated at the LHC by searching for the Higgs boson and eventually studying its properties. Recent results in the search for the SM Higgs Boson at the LHC indicates the observation of a new particle [1, 2], which is a neutral boson with a mass  $M \sim 125$  GeV. In this spectacular new observation, as well as in previous searches and studies, the preferred search mode involves Higgs boson production via gluon fusion followed by the rare decay into a pair of photons. Therefore, it is essential to count on an accurate theoretical description of the various kinematical distributions associated to the production of pairs of prompt photons with large invariant mass.

We are interested in the process  $pp \rightarrow \gamma\gamma X$ , which, at the lowest order in perturbative QCD, occurs *via* the quark annihilation subprocess  $q\bar{q} \rightarrow \gamma\gamma$ . The QCD corrections at the next-to-leading order (NLO) in the strong coupling  $\alpha_s$  involve the quark annihilation channel and a new partonic channel, *via* the subprocess  $qg \rightarrow \gamma\gamma q$ . These corrections have been computed and

implemented in the fully-differential Monte Carlo codes DIPHOX [3], 2gammaMC [4] and MCFM [5]. A calculation that includes the effects of transverse-momentum resummation is implemented in RESBOS [6]. At the next-to-next-to-leading order (NNLO), the  $gg$  channel starts to contribute, and the large gluon–gluon luminosity makes this channel sizeable. Part of the contribution from this channel, the so called *box contribution*, was computed long ago [7] and its size turns out to be comparable to the lowest-order result.

Besides their *direct* production from the hard subprocess, photons can also arise from fragmentation subprocesses of QCD partons. The computation of fragmentation subprocesses requires (poorly known) non-perturbative information, in the form of parton fragmentation functions of the photon. The complete NLO single- and double-fragmentation contributions are implemented in DIPHOX [3]. The effect of the fragmentation contributions is sizeably reduced by the photon isolation criteria that are necessarily applied in hadron collider experiments to suppress the very large irreducible background (e.g., photons that are faked by jets or produced by hadron decays). The standard cone isolation and the ‘smooth’ cone isolation proposed by Frixione [8] are two of these criteria. The standard cone isolation is easily implemented in experiments, but it only suppresses a fraction of the fragmentation contribution. The smooth cone isolation (formally) eliminates the entire fragmentation contribution, but its experimental im-

---

*Email address:* cieri@fi.infn.it (Leandro Cieri)

plementation is still under study [9]. However, it is important to anticipate (work to appear) that in some kinematical regions (e.g for Higgs boson searches) QCD calculations that apply the standard cone and the Frixione isolation criteria give basically very similar quantitative results<sup>1</sup>.

## 2. Diphoton production at NNLO

We consider the inclusive hard-scattering reaction

$$h_1 + h_2 \rightarrow \gamma\gamma + X, \quad (1)$$

where the collision of the two hadrons,  $h_1$  and  $h_2$ , produces the diphoton system  $F \equiv \gamma\gamma$  with high invariant mass  $M_{\gamma\gamma}$ . The evaluation of the NNLO corrections to this process requires the knowledge of the corresponding partonic scattering amplitudes with  $X = 2$  partons (at the tree level [10]),  $X = 1$  parton (up to the one-loop level [11]) and no additional parton (up to the two-loop level [12]) in the final state. The implementation of the separate scattering amplitudes in a complete NNLO (numerical) calculation is severely complicated by the presence of infrared (IR) divergences that occur at intermediate stages. The  $q_T$  subtraction formalism [13] is a method that handles and cancels these unphysical IR divergences up to the NNLO. The formalism applies to generic hadron collision processes that involve hard-scattering production of a colourless high-mass system  $F$ . Within that framework [13], the corresponding cross section is written as:

$$d\sigma_{(N)NLO}^F = \mathcal{H}_{(N)NLO}^F \otimes d\sigma_{LO}^F + \left[ d\sigma_{(N)LO}^{F+jets} - d\sigma_{(N)LO}^{CT} \right], \quad (2)$$

where  $d\sigma_{(N)LO}^{F+jets}$  represents the cross section for the production of the system  $F$  plus jets at (N)LO accuracy<sup>2</sup>, and  $d\sigma_{(N)LO}^{CT}$  is a (IR subtraction) counterterm whose explicit expression [15] is obtained from the resummation program of the logarithmically-enhanced contributions to  $q_T$  distributions. The ‘coefficient’  $\mathcal{H}_{(N)NLO}^F$ , which also compensates for the subtraction of  $d\sigma_{(N)LO}^{CT}$ , corresponds to the (N)NLO truncation of the process-dependent perturbative function

$$\mathcal{H}^F = 1 + \frac{\alpha_S}{\pi} \mathcal{H}^{F(1)} + \left( \frac{\alpha_S}{\pi} \right)^2 \mathcal{H}^{F(2)} + \dots \quad (3)$$

<sup>1</sup>The use of the same parameters in both criteria is understood.

<sup>2</sup>In the case of diphoton production, the NLO calculation of  $d\sigma_{NLO}^{\gamma\gamma+jets}$  was performed in Ref.[14].

The NLO calculation of  $d\sigma^F$  requires the knowledge of  $\mathcal{H}^{F(1)}$ , and the NNLO calculation also requires  $\mathcal{H}^{F(2)}$ . The general structure of  $\mathcal{H}^{F(1)}$  is explicitly known [16]; exploiting the explicit results of  $\mathcal{H}^{F(2)}$  for Higgs [13, 17] and vector boson [18] production, we have generalized the process-independent relation of Ref. [16] to the calculation of the NNLO coefficient  $\mathcal{H}^{F(2)}$ .

## 3. Quantitative results

We have performed our fully-differential NNLO calculation [19] of diphoton production according to Eq. (2). The NNLO computation is encoded in a parton level Monte Carlo program, in which we can implement arbitrary IR safe cuts on the final-state photons and the associated jet activity. We concentrate on the direct production of diphotons, and we rely on the smooth cone isolation criterion [8]. Considering a cone of radius  $r = \sqrt{(\Delta\eta)^2 + (\Delta\phi)^2}$  around each photon, we require the total amount of hadronic (partonic) transverse energy  $E_T$  inside the cone to be smaller than  $E_{Tmax}^{had}(r)$ ,

$$E_T < E_{Tmax}^{had}(r) \equiv E_{Tmax} \left( \frac{1 - \cos r}{1 - \cos R} \right)^n, \quad (4)$$

where  $E_{Tmax}$  can be a fixed value or a fraction of the transverse momentum of the photon ( $E_{Tmax} = \epsilon_\gamma p_T^\gamma$ , with  $0 < \epsilon_\gamma \leq 1$ ); the isolation criterion  $E_T < E_{Tmax}^{had}(r)$  has to be fulfilled for all cones with  $r \leq R$ . We use the MSTW 2008 [20] sets of parton distributions, with densities and  $\alpha_S$  evaluated at each corresponding order, and we consider  $N_f = 5$  massless quarks/antiquarks and gluons in the initial state. The default renormalization ( $\mu_R$ ) and factorization ( $\mu_F$ ) scales are set to the value of the invariant mass of the diphoton system,  $\mu_R = \mu_F = M_{\gamma\gamma}$ . The QED coupling constant  $\alpha$  is fixed to  $\alpha = 1/137$ .

To present some quantitative results, we consider diphoton production at the LHC ( $\sqrt{s} = 14$  TeV). We apply typical kinematical cuts used by ATLAS and CMS Collaborations in their Higgs boson search studies. We require the harder and the softer photon to have transverse momenta  $p_T^{\text{harder}} \geq 40$  GeV and  $p_T^{\text{softer}} \geq 25$  GeV, respectively. The rapidity of both photons is restricted to  $|y_\gamma| \leq 2.5$ , and the invariant mass of the diphoton system is constrained to lie in the range  $20 \text{ GeV} \leq M_{\gamma\gamma} \leq 250 \text{ GeV}$ . The isolation parameters are set to the values  $\epsilon_\gamma = 0.5$ ,  $n = 1$  and  $R = 0.4$ . Performing the QCD computation, we observe [19] that the value of the cross section remarkably increases with the perturbative order of the calculation. This increase is mostly due to the use of *very asymmetric* (unbalanced) cuts on

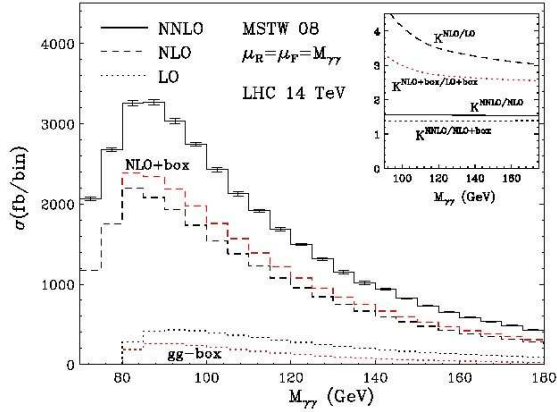


Figure 1: Invariant mass distribution of the photon pair at the LHC ( $\sqrt{s} = 14$  TeV): LO (dots), NLO (dashes) and NNLO (solid) results. We also present the results of the box and NLO+box contributions. The inset plot shows the corresponding K-factors.

the photon transverse momenta. At the LO, kinematics implies that the two photons are produced with equal transverse momentum and, thus, both photons should have  $p_T^\gamma \geq 40$  GeV. At higher orders, the final-state radiation of additional partons opens a new region of the phase space, where  $40 \text{ GeV} \geq p_T^{\text{softer}} \geq 25$  GeV. Since photons can copiously be produced with small transverse momentum [19], the cross section receives a sizeable contribution from the enlarged phase space region. This effect is further enhanced by the opening of a new large-luminosity partonic channel at each subsequent perturbative order. In Fig. 1 we show the LO, NLO and NNLO invariant mass distributions at the default scales. We also plot the gluonic *box contribution* (computed with NNLO parton distributions) and its sum with the full NLO result. The inset plot shows the K-factors defined as the ratio of the cross sections at two subsequent perturbative orders. We note that  $K^{\text{NNLO}/\text{NLO}}$  is sensibly smaller than  $K^{\text{NLO}/\text{LO}}$ , and this fact indicates an improvement in the convergence of the perturbative expansion. We find that about 30% of the NNLO corrections is due to the *gg channel* (the *box contribution* is responsible for more than half of it), while almost 60% still arises from the next-order corrections to the *qg channel*. The NNLO calculation includes the perturbative corrections from the entire phase space region (in particular, the next-order correction to the dominant *qg channel*) and the contributions from all possible partonic channels (in particular, a fully-consistent treatment of the *box contribution* to the *gg channel*<sup>3</sup>). Owing to

<sup>3</sup>The calculation [4] of the next-order gluonic corrections to the *box contribution* indicates an increase of the NNLO result by less than 10% if  $M_{\gamma\gamma} \geq 100$  GeV.

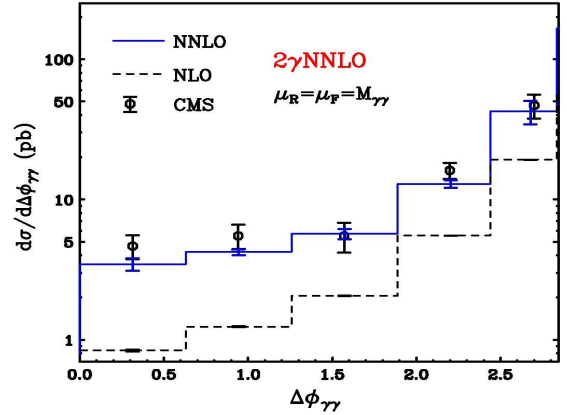


Figure 2: Diphoton cross section as a function of the azimuthal separation of the two photons. Data from CMS [21] ( $\sqrt{s} = 7$  TeV) are compared to the NNLO calculation [19].

these reasons, the NNLO result can be considered a reliable estimate of direct diphoton production, although further studies (including independent variations of  $\mu_R$  and  $\mu_F$ , and detailed analyses of kinematical distributions) are necessary to quantify the NNLO theoretical uncertainty.

Recent results from the LHC [21, 22] and the Tevatron [23] show some discrepancies between the data and NLO theoretical calculations of diphoton production. Basically, discrepancies were found in kinematical regions where the NLO calculation is *effectively* a LO theoretical description of the process. Such phase space regions (away from the back-to-back configuration) are accessible at NLO for the first time, due to the final-state radiation of the additional parton<sup>4</sup>. Figure 2 shows a measurement by CMS [21], of the diphoton cross section as a function of the azimuthal angle  $\Delta\phi_{\gamma\gamma}$  between the photons. The data are compared with our NLO and NNLO calculations [19]. The acceptance criteria used in this analysis ( $\sqrt{s} = 7$  TeV) require:  $p_T^{\text{harder}} \geq 23$  GeV and  $p_T^{\text{softer}} \geq 20$  GeV. The rapidity of both photons is restricted to  $|y_\gamma| \leq 2.5$ , and the invariant mass of the diphoton system is constrained to be  $M_{\gamma\gamma} > 80$  GeV. The isolation parameters have the values  $\epsilon_\gamma = 0.05$ ,  $n = 1$  and  $R = 0.4$ .

The histograms in Fig. 2 show that the NNLO QCD results remarkably improve the theoretical description of the CMS data throughout the entire range of  $\Delta\phi_{\gamma\gamma}$ .

In Figure 3, we present the invariant mass distribution for diphoton production at the Tevatron ( $\sqrt{s} =$

<sup>4</sup>The low-mass region ( $M_{\gamma\gamma} \leq 80 \text{ GeV}$ ) in Figure 1 also belongs to this case.

1.96 TeV) calculated at NNLO, compared with a measurement performed by CDF [23]. The acceptance criteria in this case require:  $p_T^{\text{harder}} \geq 17$  GeV and  $p_T^{\text{softer}} \geq 15$  GeV. The rapidity of both photons is restricted to  $|y_\gamma| \leq 1$ . The isolation parameters are set to the values  $E_{T \text{ max}} = 2$  GeV,  $n = 1$  and  $R = 0.4$ , and the minimum angular separation between the two photons is  $R_{\gamma\gamma} = 0.4$ . Though in this case the in-

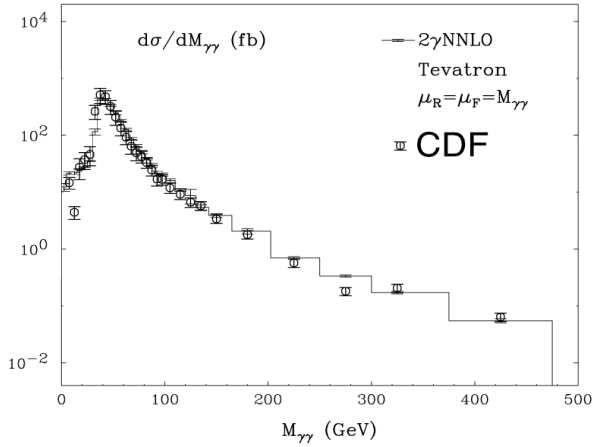


Figure 3: Diphoton cross section as a function of the invariant mass of the two photons. Data from CDF [23] ( $\sqrt{s} = 1.96$  TeV) are compared to the NNLO calculation.

crease from the LO to the NLO result is considerably smaller than at the LHC [19], the NNLO QCD corrections still improve remarkably the theoretical description of the CDF data, in particular in the low mass region ( $M_{\gamma\gamma} \leq 2p_T^{\text{harder}} = 34$  GeV).

We note that the CMS and CDF data are obtained by using the standard cone isolation criterion and the constraint in Eq. (4) is applied only to the cone of radius  $r = R$ . Since the smooth isolation criterion used in our calculation (we apply Eq. (4) for all cones with  $r \leq R$ ) is stronger than the photon isolation used by CMS and CDF, we remark that our NLO and NNLO results cannot overestimate the corresponding theoretical results for the experimental isolation criterion.

The results illustrated in this contribution show that the NNLO description of diphoton production is essential to understand the phenomenology associated to this process, and therefore, the NNLO calculation is a relevant tool to describe the main background for Higgs boson searches and studies.

## Acknowledgements

I would like to thank Stefano Catani and Daniel de Florian for helpful comments. This work was supported by the INFN and the Research Executive Agency (REA) of the European Union under the Grant Agreement number PITN-GA-2010-264564 (LHCPhenoNet).

## References

- [1] S. Chatrchyan *et al.* [CMS Collaboration], [arXiv:1207.7235 [hep-ex]].
- [2] G. Aad *et al.* [ATLAS Collaboration], [arXiv:1207.7214 [hep-ex]].
- [3] T. Binoth, J. P. Guillet, E. Pilon and M. Werlen, Eur. Phys. J. **C16**, 311 (2000).
- [4] Z. Bern, L. J. Dixon and C. Schmidt, Phys. Rev. **D66**, 074018 (2002).
- [5] J. M. Campbell, R. K. Ellis and C. Williams, JHEP **1107**, 018 (2011).
- [6] C. Balazs, E. L. Berger, P. M. Nadolsky and C. -P. Yuan, Phys. Rev. **D76**, 013009 (2007).
- [7] D. A. Dicus and S. S. D. Willenbrock, Phys. Rev. **D37**, 1801 (1988).
- [8] S. Frixione, Phys. Lett. **B429**, 369 (1998).
- [9] R. Blair, B. Brelief, F. Bucci, S. Chekanov, M. Stockton and M. Tripania, CERN-OPEN-2011-041, (2011).
- [10] V. D. Barger, T. Han, J. Ohnemus and D. Zeppenfeld, Phys. Rev. **D41**, 2782 (1990); V. Del Duca, W. B. Kilgore and F. Maltoni, Nucl. Phys. **B566**, 252 (2000).
- [11] Z. Bern, L. J. Dixon and D. A. Kosower, Nucl. Phys. **B437**, 259 (1995); A. Signer, Phys. Lett. **B357**, 204 (1995).
- [12] C. Anastasiou, E. W. N. Glover and M. E. Tejeda-Yeomans, Nucl. Phys. **B629**, 255 (2002).
- [13] S. Catani and M. Grazzini, Phys. Rev. Lett. **98**, 222002 (2007).
- [14] V. Del Duca, F. Maltoni, Z. Nagy and Z. Trocsanyi, JHEP **0304**, 059 (2003).
- [15] G. Bozzi, S. Catani, D. de Florian and M. Grazzini, Nucl. Phys. **B737**, 73 (2006).
- [16] D. de Florian and M. Grazzini, Phys. Rev. Lett. **85**, 4678 (2000), Nucl. Phys. **B616**, 247 (2001).
- [17] S. Catani and M. Grazzini, Eur. Phys. J. C **72** (2012) 2013 [arXiv:1106.4652 [hep-ph]].
- [18] S. Catani, L. Cieri, G. Ferrera, D. de Florian and M. Grazzini, Phys. Rev. Lett. **103**, 082001 (2009).
- [19] S. Catani, L. Cieri, D. de Florian, G. Ferrera and M. Grazzini, Phys. Rev. Lett. **108** (2012) 072001.
- [20] A. D. Martin, W. J. Stirling, R. S. Thorne and G. Watt, Eur. Phys. J. **C63**, 189 (2009).
- [21] S. Chatrchyan *et al.* [CMS Collaboration], arXiv:1110.6461 [hep-ex].
- [22] G. Aad *et al.* [ATLAS Collaboration], Phys. Rev. D **85** (2012) 012003.
- [23] T. Aaltonen *et al.* [CDF Collaboration], Phys. Rev. D **84** (2011) 052006.